Volume 59
Number 49
21 June 2023
Pages 7473–7664

ChemComm

Chemical Communications

rsc.li/chemcomm

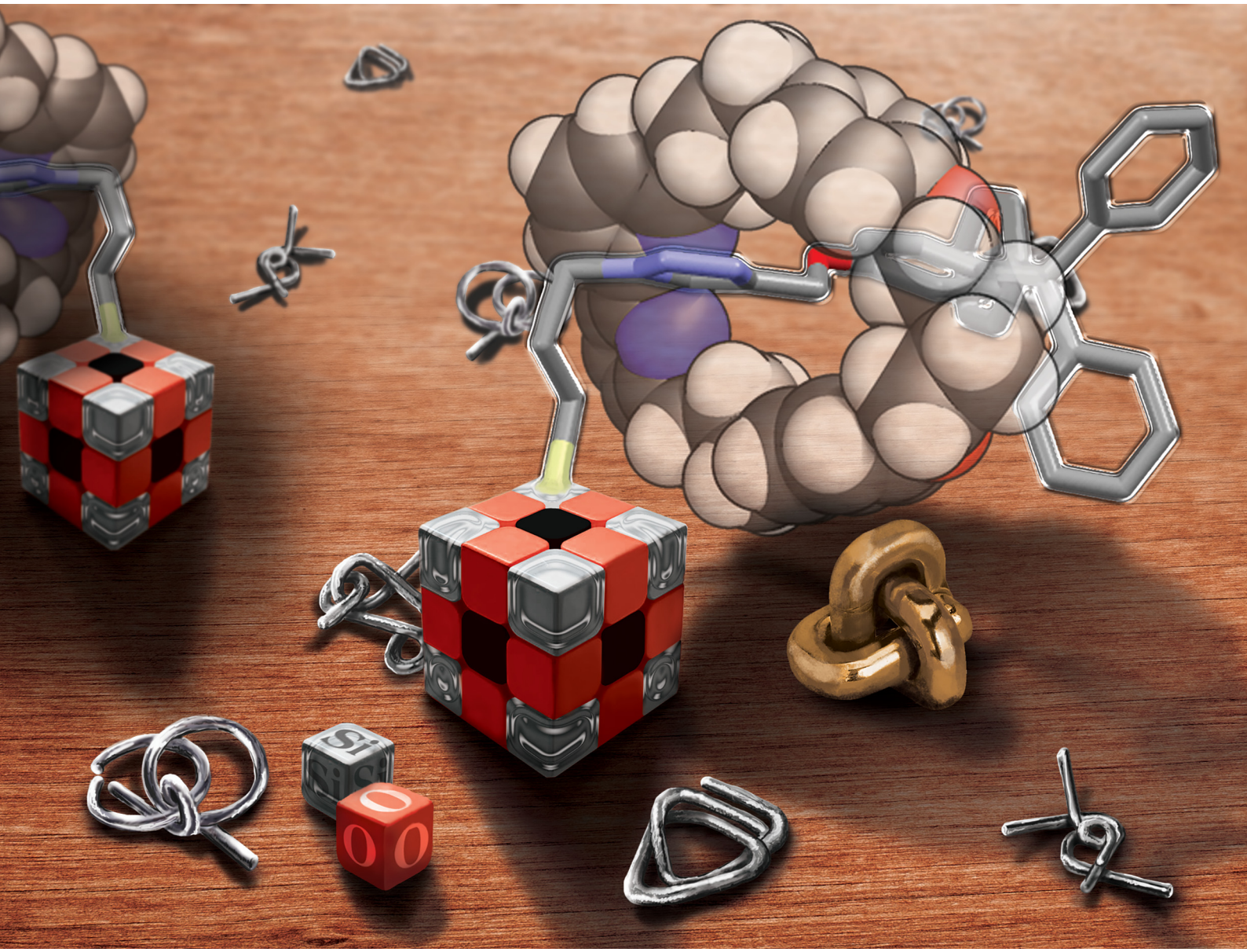

ISSN 1359-7345

ROYAL SOCIETY OF CHEMISTRY

COMMUNICATION

Łukasz John, Bartosz Szyszko *et al.*

POSSaxanes: active-template synthesis of organic–inorganic rotaxanes incorporating cubic silsesquioxane stoppers

ChemComm

COMMUNICATION

View Article Online
View Journal | View Issue

Cite this: *Chem. Commun.*, 2023, 59, 7579

Received 10th April 2023,
Accepted 9th May 2023

DOI: 10.1039/d3cc01706k

rsc.li/chemcomm

POSSaxanes: active-template synthesis of organic–inorganic rotaxanes incorporating cubic silsesquioxane stoppers†

Rafał A. Grzelczak, Anna Władyczyn, Agata Białońska, Łukasz John * and Bartosz Szyszko *

The CuAAC active-template approach was exploited to construct rotaxanes incorporating cage-like silsesquioxane stoppers, namely, POSSaxanes. The compounds were characterized in the solution and solid state, providing the unprecedented molecular structures of POSS-incorporating rotaxanes.

The construction of hybrid systems merging organic and inorganic functionalities has emerged as an exciting approach allowing the formation of molecules and materials with novel functions.[1] A unique group of such composites is mechanically interlocked materials that were demonstrated not only to present the features expected of the individual components, but to benefit from the novel, synergistic effects arising from the mechanical bond presence.[2] In this context, rotaxanes comprise a group of particularly well-studied, mechanically interlocked molecules, which have demonstrated applications in areas spreading from molecular machines and motors, to stimuli-responsive polymers, and drug delivery systems.[3]

The alluring class of rotaxanes includes organic–inorganic hybrids, which, depending on the design, contain an inorganic macrocycle,[1,4,5] a metal-based host,[6] or an axle with the metal cation incorporated into the thread[7] as its structural element,[8] or as the motif organizing organic ligands into the coordination compound constituting the stopper(s).[9,10] The emerging group of mechanically interlocked materials comprises MOFs embedding interlocked components,[11] and systems with the thread attached to the metal, or metal oxide nanoparticles,[12,13] or graphene.[14]

Polyhedral Oligomeric Silsesquioxanes (POSSs) are a group of hybrid building blocks of subnanometer and nanometer dimensions exploited for constructing novel materials with tailored functions.[15] Within the vast group of cage-like silsesquioxanes, the cubic cages of general formula $(RSiO_{1.5})_8$ are particularly attractive due to their intrinsic properties and facile functionalization. POSSs have found applications in catalysis, nanomedicine, and materials chemistry, where they were exploited as porous media, components of nanocomposites, and molecular encapsulants.[16]

Herein we report the facile synthesis of POSS-stoppered rotaxanes, *i.e.*, POSSaxanes, based on the active template CuAAC approach. Active template (AT) synthesis is considered one of the most powerful tools for constructing MIMs. The critical element of the AT method relies upon the metal cation, which serves a dual purpose, functioning both as a template that organizes the components into the threaded architecture and as a catalyst taking part in the formation of the covalent bond resulting in the interlocked structure.[17,18] Our interest in exploiting cubic silsesquioxanes for rotaxane synthesis stems from several reasons. The POSS cages are synthetically accessible, allowing for gram scale preparation in a relatively short time, and can be considered nanometer-sized stoppers, whose dimensions can be easily tuned with the appropriate substitution pattern of the silicon-based vertices. Notably, materials functionalized with cage-like silsesquioxanes have demonstrated improved resistance to thermal degradation and oxidative stability.[19] Despite the evident benefits of the POSS motif, it was only incidentally exploited for synthesizing polypseudorotaxanes based on the cyclodextrin macrocycle.[20,21]

The POSSaxanes synthesis was envisaged to exploit the silsesquioxane precursors equipped with a single reactive arm terminated with either alkyne or azide functionality and seven chemically inert (iso-butyl or phenyl) substituents at the cube vertices, providing steric hindrance (Scheme 1). Once reacted in the presence of the macrocycle, these half-axle components were intended to introduce the POSS-stopper(s) into the rotaxane molecule. The essential starting materials for the half-axle syntheses, namely the open cages **1a**/**b**, were either commercially available or could be easily obtained from the reaction of trimethoxysilane **S14** with an aqueous solution of sodium

University of Wrocław, Faculty of Chemistry, 14 F. Joliot-Curie St., 50-383 Wrocław, Poland. E-mail: lukasz.john@uwr.edu.pl, bartosz.szyszko@uwr.edu.pl

† Electronic supplementary information (ESI) available. CCDC 2249743 and 2249744. For ESI and crystallographic data in CIF or other electronic format see DOI: https://doi.org/10.1039/d3cc01706k

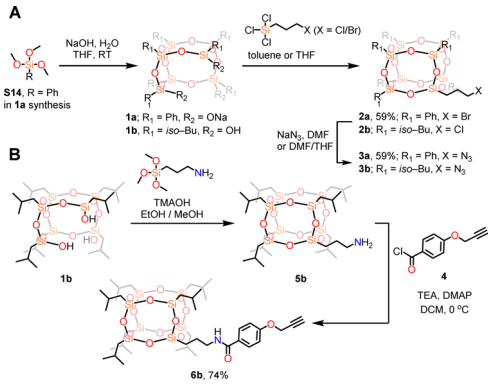

Scheme 1 Synthesis of POSS-incorporating (A) azides and (B) alkyne precursors.

hydroxide in THF. The azides **3a/b** were synthesized by the corner capping of **1a/b** with 3-halopropyl(trichlorosilane), followed by azidation of the initially formed **2a/b.** The corner-capping of the commercially available triol **1b** with 3-aminopropyl(trimethoxysilane) yielded amine **5b**, which upon reaction with 4-propargyloxybenzoic acid chloride **4** in the presence of TEA/DMAP formed alkyne **6b** in 74% yield. The alkyne **7** and azide **8** were additionally synthesized to target POSSaxanes stoppered with POSS at one end and a tetrahedral trityl-group at the other.

The crucial step in the rotaxane synthesis was realized through the active template copper(I)-catalyzed azide–alkyne cycloaddition between the half-axle components, namely the POSS-terminated alkyne or azides, in the presence of the macrocyclic compound (Scheme 2). In order to determine the versatility of the developed cage-like stoppers, the POSSaxane syntheses were evaluated by exploiting the bipyridine – **A**,[22] and pyridine-

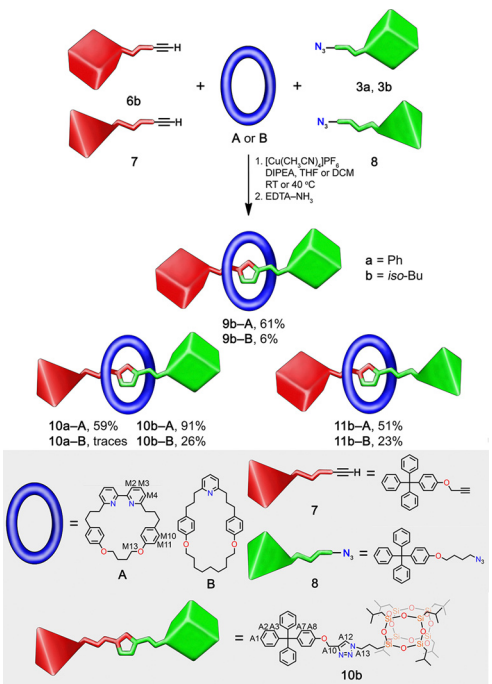

Scheme 2 The CuAAC active-template synthesis of POSSaxanes.

incorporating **B** macrocycles[23] reported by Goldup and Leigh, respectively. The two macrocyclic compounds differ in the incorporated coordinating motif but have cavities of comparable size, as defined by the smallest macrocyclic circuit composed of 26 (**A**) and 28 (**B**) atoms.

Three types of rotaxanes were targeted, incorporating the silsesquioxane stopper at the azide or alkyne side of the triazole moiety and those with the POSS groups terminating both ends of the axle (Scheme 2). The conditions developed for bipyridine macrocycle-based POSSaxanes required carrying out the reaction of **A** with a slight excess (1.2 equiv.) of azide **3a**/**b**/**8** and alkyne **6b**/**7** in THF or DCM in the presence of a catalytic amount (0.25 equiv.) of tetrakis(acetonitrile)copper(I) hexafluorophosphate and diisopropylethylamine (DIPEA, 1 equiv.) for *ca.* 20 hours. After the reaction workup and chromatographic separation, POSSaxanes **9b-A**, **10b-A**, and **11b-A**, incorporating iso-Bu$_7$-POSS stoppers, were isolated in 51–91% yield. The synthesis of POSSaxanes stoppered with Ph$_7$-POSS groups required harsher conditions, namely carrying out the reaction at elevated temperature (40 °C) and for a longer time (*ca.* 40 hours). The POSSaxane **10a-A** could be isolated following the modified synthetic protocol with a 59% yield.

The synthesis of POSSaxanes based on the pyridine-incorporating macrocycle **B** required reevaluating the previously developed conditions. In order to improve the yield of target compounds, THF solvent was replaced with poorly coordinating DCM, and the reaction time was elongated to 48–72 hours. Furthermore, a larger (2 equiv.) excess of half-axle components had to be used in some cases. Despite these modifications, the yields of **9b-B**, **10b-B**, and **11b-B** were visibly lower than their bipyridine-incorporating analogs, reaching only 6–26%. In the extreme case of the Ph$_7$-POSS-incorporating **10a-B**, only traces of the target compound were detected in the reaction mixture. This result can be rationalized concerning the steric hindrance of the phenyl groups in the Ph$_7$-POSS azide **3a** hampering the effective formation of the intermediate copper(I)-azide–alkyne macrocyclic complex.

The formation of **10b-A**, which can be considered a representative example of a POSSaxane group, is evident upon comparing its ^{1}H NMR resonances with the spectra of the respective macrocycle **A** and independently synthesized thread **10b** (Fig. 1; see ESI† for others). In particular, the resonances M2, M3, and M4 of the bipyridine unit were slightly up-field shifted from 7.61–7.55, and 7.09 ppm in the spectrum of **A** to 7.55, 7.35, and 7.03 ppm for **10b-A**, respectively. The characteristic triazole CH singlet of the **10b** thread underwent a downfield shift from 7.55 ppm to 8.30 ppm in **10b-A**, resulting from the CH$\cdots$N hydrogen bonding between the triazole linker of the axle and bipyridine of the macrocycle.[24] The incorporation of the POSS stopper was also evident from the presence of the characteristic set of resonances corresponding to the protons of iso-butyl groups at the POSS vertices in the ^{1}H NMR spectrum of **10b-A** (Fig. S31, ESI†). In addition, the ^{29}Si NMR spectrum demonstrated four overlapping resonances in the −66.0 to −67.0 ppm region, corresponding to the silicon vertices of the POSS stopper (inset in Fig. 1B).

Remarkably, the molecular structures of two POSSaxanes **10a-A** and **10b-A** were determined in the solid state by means of

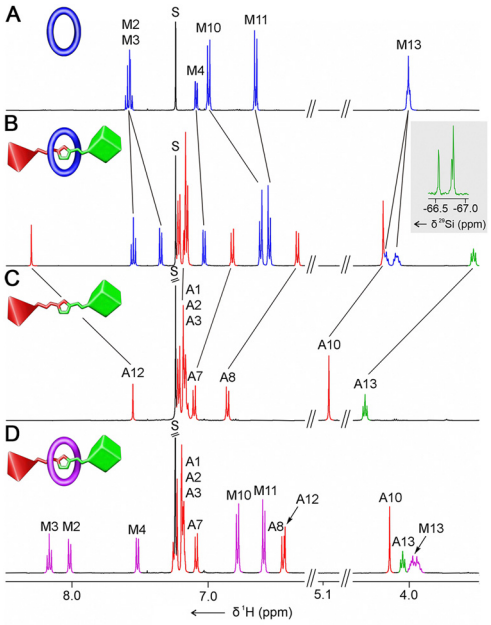

Fig. 1 The ^{1}H NMR spectra ($CDCl_3$, 300 K, 500 MHz) of (A) **A**, (B) **10b-A**, (C) **10b**, and (D) **10b-A·(TFAH)$_n$**. The inset in B demonstrates the ^{29}Si NMR spectrum. The aliphatic region was omitted for clarity. The resonance numbering is shown in Scheme 2.

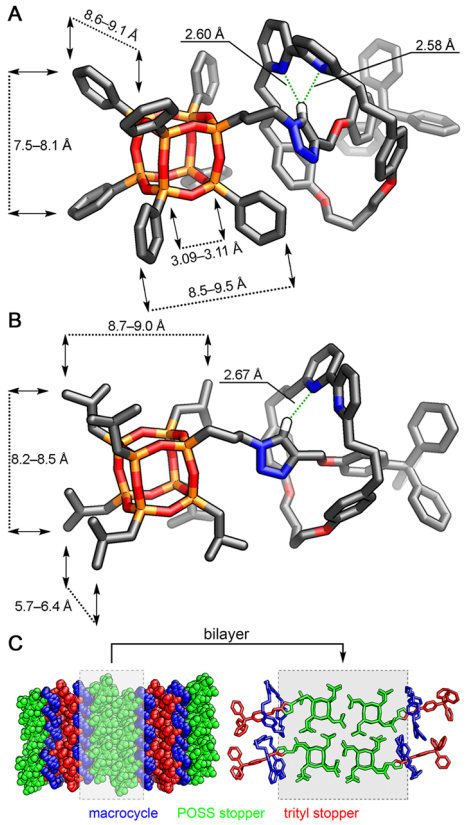

Fig. 2 The X-ray molecular structure of (A) **10a-A** and (B) **10b-A**. Protons, except for the CH involved in HB, were omitted for clarity. (C) The packing diagram of **10b-A**.

XRD studies (Fig. 2). The monocrystals of **10a-A** were grown by slow evaporation of THF/hexane solution, whereas those of **10b-A** were obtained by diffusion of methanol into the ethyl acetate solution of the rotaxane.

The molecular structure of **10a-A** demonstrated the rotaxane molecule composed of the macrocycle with the triazole-incorporating axle stoppered with the trityl and Ph_7-POSS units (Fig. 2A). The triazole of the thread was located close to the bipyridine of **A**, resulting in CH···N hydrogen bonds of 2.58–2.60 Å length. Although the tetrahedral trityl group provided enough steric hindrance to play a stopper role for the **A**-based rotaxane, the POSS unit's dimensions are considerably larger. Despite the fact that the Si–O–Si distances within the cage-like silsesquioxane are 3.09–3.11 Å, the substitution of the silicon vertices with phenyl rings resulted in a stopper with impressive subnanometer-to-nanometer dimensions illustrated by the edge length ranging from 7.5–9.5 Å ($C_{para\text{-}Ph}\cdots C_{para\text{-}Ph}$) to 8.4–10.8 Å ($H_{para\text{-}Ph}\cdots H_{para\text{-}Ph}$). In comparison, the iso-Bu_7-POSS stopper in **10b-A** demonstrated slightly smaller dimensions, with the edge lengths being in the range of 5.7–9.0 Å ($C_{para\text{-}Ph}\cdots C_{para\text{-}Ph}$)/7.5–10.6 Å ($H_{para\text{-}Ph}\cdots H_{para\text{-}Ph}$), depending on the orientation of the alkyl groups at the vertices (Fig. 2B). Interestingly, as shown in the packing diagram of **10b-A**, the molecules of the POSSaxane are arranged in the crystal network into trityl-macrocycle-POSS···POSS-macrocycle-trityl bilayers (Fig. 2C). This organization increased the contact surface area between the iso-butyl groups on one end of the rotaxane molecules and appropriately oriented phenyl rings on the other, enforcing the layer stabilization through intermolecular van der Waals and edge-to-face π–π stacking interactions.

Considering the potential applications of POSSaxanes for constructing new mechanically interlocked materials, their stability in the solution and solid-state was investigated. The prolonged heating of **10b-A** in toluene at 100 °C did not result in degradation of the POSS-stopper nor rotaxane dethreading (Fig. S122, ESI†).

The acidification of **10b-A** with trifluoroacetic acid yielded cationic **10b-A·(TFAH)$_n$** as the sole product, as monitored by ^{1}H NMR titration (Fig. S52, ESI†). The ^{1}H NMR spectrum of **10b-A·(TFAH)$_n$** demonstrated the features expected of a cationic rotaxane, with the characteristic up-field shift of the triazole proton resonance from 8.30 ppm (**10b-A**) to 6.43 ppm, being a result of disruption of the hydrogen bond network upon bipyridine protonation (Fig. 1D). In addition, the macrocycle's M2, M3, and M4 signals were markedly down-field shifted to 8.03, 8.16, and 7.51 ppm. Upon the addition of TEA to the sample of **10b-A·(TFAH)$_n$**, the rotaxane **10b-A** was restored, with no dethreading or degradation products observed in the solution (Fig. S126, ESI†).

As the cubic silsesquioxane was previously demonstrated to undergo rearrangement reactions in the presence of fluoride anions, the stability of POSSaxanes in the presence of TBAF was investigated.[25] Unexpectedly, the gradual increase of fluoride concentration in the solution of **10b-A** in DCM-d_2 resulted in new resonances (Fig. S123 and S124, ESI†). Upon the addition of 30 equiv. of TBAF, the resonances of the macrocycle **A** were detected, indicating that the rotaxane underwent dethreading. The MS analysis of the reaction mixture indicated the liberation

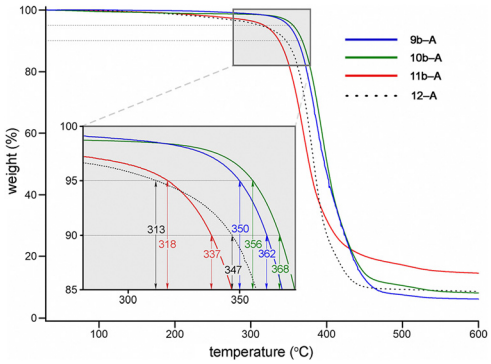

Fig. 3 The TGA curves of **12-A**, **9b-A**, **10b-A**, and **11b-A**.

of the macrocycle **A** and the formation of several silicon-containing degradation products that could not be unambiguously identified (Fig. S143, ESI†).

Eventually, the thermal stability of POSSaxanes was studied in the solid state employing thermogravimetric analysis (TGA) (Fig. 3, S144–S152, ESI†). All POSSaxanes incorporating the macrocycle **A** and the reference compound **12-A** incorporating two trityl stoppers displayed similar thermal degradation profiles. The temperature values at 5% and 10% of weight loss were evaluated to determine the effect of the POSS moiety's presence. The installment of the POSS stoppers affected the degradation temperature of the rotaxanes. The $T_{5\%}$ and $T_{10\%}$ of **9b-A** and **10b-A** were increased to 350/362 °C (**9b-A**) and 356/368 °C (**10b-A**), in comparison to 313/347 °C detected for the reference **12-A**. At the same time, the rotaxanes incorporating the **6b**-originating stopper demonstrated decreased thermal stability, likely due to the presence of the amide functional group. In the case of **B**-based POSSaxanes, the modification of thermal stability was negligible (Fig. S149–S152, ESI†). Although the effect of the POSS stopper on the thermal stability of some rotaxanes is apparent, the inherent chemical structure of each MIM, in particular the presence of specific functional groups, must be taken into account to design a material with improved thermal stability characteristics.

Facile syntheses of cubic silsesquioxanes and their subnanometer-to-nanometer dimensions encouraged their exploitation to construct novel rotaxanes using the active template approach. The POSS-terminated rotaxanes were obtained with good-to-excellent yields indicating that the vertices-substituted silicon-containing cages can be considered a valuable group of stoppers, especially when the large macrocycles are to be exploited.[26] POSSaxanes demonstrated stability in the solution at elevated temperature and under acidic conditions, yet the cleavage of POSS units in the presence of fluoride resulted in dethreading liberating the macrocyclic component. Incorporating the silsesquioxane cage into the rotaxane architecture was demonstrated to improve the thermal stability of the compounds in the solid state, encouraging their exploitation for the construction of novel functional, mechanically interlocked materials. Furthermore, POSSaxanes can be considered a unique group of Polyhedral Oligomeric Silsesquioxanes wherein a considerable part of the molecule is sterically protected by introducing MIM architecture. It is envisaged that such a modification of the POSS framework might influence the accessibility of silicon atoms at the cage corners and face, eventually affecting their reactivity.

The National Science Centre of Poland supported this work upon grant agreement no. 2020/38/E/ST4/00024.

Conflicts of interest

There are no conflicts to declare.

Notes and references

1 E. K. Brechin and L. Cronin, *Angew. Chem., Int. Ed.*, 2009, **48**, 6948–6949.
2 S. Mena-Hernando and E. M. Pérez, *Chem. Soc. Rev.*, 2019, **48**, 5016–5032.
3 M. Xue, Y. Yang, X. Chi, X. Yan and F. Huang, *Chem. Rev.*, 2015, **115**, 7398–7501.
4 C.-F. Lee, D. A. Leigh, R. G. Pritchard, D. Schultz, S. J. Teat, G. A. Timco and R. E. P. Winpenny, *Nature*, 2009, **458**, 314–318.
5 G. A. Timco, A. Fernandez, A. K. Kostopoulos, J. F. Charlton, S. J. Lockyer, T. R. Hailes, R. W. Adams, E. J. L. McInnes, F. Tuna, I. J. Vitorica-Yrezabal, G. F. S. Whitehead and R. E. P. Winpenny, *Angew. Chem., Int. Ed.*, 2018, **57**, 10919–10922.
6 P. J. Altmann and A. Pöthig, *Angew. Chem., Int. Ed.*, 2017, **56**, 15733–15736.
7 Y. Suzaki, T. Taira, K. Osakada and M. Horie, *Dalton Trans.*, 2008, 4823.
8 B. A. Blight, X. Wei, J. A. Wisner and M. C. Jennings, *Inorg. Chem.*, 2007, **46**, 8445–8447.
9 S. J. Loeb and J. A. Wisner, *Chem. Commun.*, 1998, 2757–2758.
10 D. J. Hoffart and S. J. Loeb, *Angew. Chem., Int. Ed.*, 2005, **44**, 901–904.
11 V. N. Vukotic, K. J. Harris, K. Zhu, R. W. Schurko and S. J. Loeb, *Nat. Chem.*, 2012, **4**, 456–460.
12 A. Ulfkjær, F. W. Nielsen, H. Al-Kerdi, T. Ruβ, Z. K. Nielsen, J. Ulstrup, L. Sun, K. Moth-Poulsen, J. Zhang and M. Pittelkow, *Nanoscale*, 2018, **10**, 9133–9140.
13 B. Long, K. Nikitin and D. Fitzmaurice, *J. Am. Chem. Soc.*, 2003, **125**, 15490–15498.
14 C. Jia, H. Li, J. Jiang, J. Wang, H. Chen, D. Cao, J. F. Stoddart and X. Guo, *Adv. Mater.*, 2013, **25**, 6752–6759.
15 R. M. Laine and M. F. Roll, *Macromolecules*, 2011, **44**, 1073–1109.
16 D. B. Cordes, P. D. Lickiss and F. Rataboul, *Chem. Rev.*, 2010, **110**, 2081–2173.
17 V. Aucagne, K. D. Hänni, D. A. Leigh, P. J. Lusby and D. B. Walker, *J. Am. Chem. Soc.*, 2006, **128**, 2186–2187.
18 M. Denis and S. M. Goldup, *Nat. Rev. Chem.*, 2017, **1**, 0061.
19 D. Zhang, R. Yang, Z. Qin and W. Zhang, *J. Therm. Anal. Calorim.*, 2023, **148**, 2345–2355.
20 Y. Ni and S. Zheng, *J. Polym. Sci., Part A: Polym. Chem.*, 2007, **45**, 1247–1259.
21 J. Huang, X. Li, T. Lin, C. He, K. Yi Mya, Y. Xiao and J. Li, *J. Polym. Sci., Part B: Polym. Phys.*, 2004, **42**, 1173–1180.
22 J. E. M. Lewis, R. J. Bordoli, M. Denis, C. J. Fletcher, M. Galli, E. A. Neal, E. M. Rochette and S. M. Goldup, *Chem. Sci.*, 2016, **7**, 3154–3161.
23 V. Aucagne, J. Berná, J. D. Crowley, S. M. Goldup, K. D. Hänni, D. A. Leigh, P. J. Lusby, V. E. Ronaldson, A. M. Z. Slawin, A. Viterisi and D. B. Walker, *J. Am. Chem. Soc.*, 2007, **129**, 11950–11963.
24 Y. Kawasaki, S. Rashid, K. Ikeyatsu, Y. Mutoh, Y. Yoshigoe, S. Kikkawa, I. Azumaya, S. Hosoya and S. Saito, *J. Org. Chem.*, 2022, **87**, 5744–5759.
25 A. R. Bassindale, Z. Liu, I. A. MacKinnon, P. G. Taylor, Y. Yang, M. E. Light, P. N. Horton and M. B. Hursthouse, *Dalton Trans.*, 2003, 2945.
26 H. Lahlali, K. Jobe, M. Watkinson and S. M. Goldup, *Angew. Chem., Int. Ed.*, 2011, **50**, 4151–4155.

